

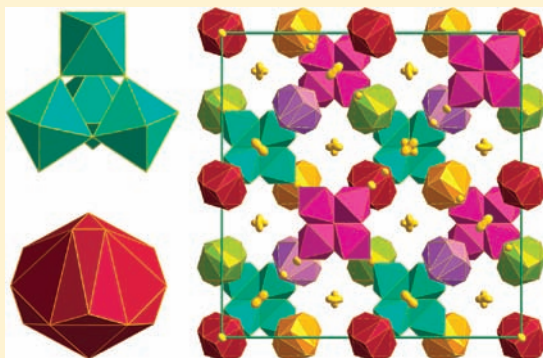
# Crystal Structure of $[\text{Al}_4(\text{OH})_6(\text{H}_2\text{O})_{12}][\text{Al}(\text{H}_2\text{O})_6]_2\text{Br}_{12}$ : A New Polyaluminum Compound

Zhong Sun,\* Hui Wang, Huijun Feng, Ying Zhang, and Shuangyan Du

College of Chemistry and Chemical Engineering, Inner Mongolia University, 235 West University Road, Hohhot 010021, China

Supporting Information

**ABSTRACT:** A vertex-shared tetrahedral  $[\text{Al}_4(\text{OH})_6(\text{H}_2\text{O})_{12}]^{6+}$  ( $\text{Al}_4$ ) and a disordered  $[\text{Al}(\text{H}_2\text{O})_6]^{3+}$  ( $\text{Al}_1$ ) that coexist in a 1:2 ratio within each unit cell were observed in the structure of  $[\text{Al}_4(\text{OH})_6(\text{H}_2\text{O})_{12}][\text{Al}(\text{H}_2\text{O})_6]_2\text{Br}_{12}$ , which crystallized in a cubic  $\text{Fd}\bar{3}m$  space group from a spontaneously hydrolyzed solution of  $\text{AlBr}_3$ . The former is composed of four  $\text{AlO}_6$  octahedra that are connected to each other by sharing three vertexes of each octahedron and form a large regular tetrahedron with ideal  $T_d$  symmetry. The central  $\text{Al}^{3+}$  ion of the latter is coordinated by 6 disordered  $\text{OH}_2$  molecules, that form a core-shell structure with ideal  $D_{3d}$  symmetry.



## INTRODUCTION

The hydrolytic chemistry of  $\text{Al}^{\text{III}}$  has received much attention in many academic fields such as geochemistry, environmental science, biochemistry, medicine, and water treatment.<sup>1–6</sup> Aluminum species play a critical role in the study of the transport and transformation of aluminum in natural water and soil. For example, Furrer et al. showed that the flocs in polluted streams come from the aggregation of  $\varepsilon\text{-K-Al}_{13}$  (one of the five Baker–Figgis–Keggin isomers,<sup>1</sup> i.e.,  $\alpha$ -,  $\beta$ -,  $\gamma$ -,  $\delta$ -, and  $\varepsilon\text{-K-Al}_{13}$ ) species.<sup>7</sup> Phillips et al. found that the  $^{17}\text{OH}_2$  exchange rates of hydroxyl ligands are extremely sensitive to subtle differences in local structure and to the Brønsted acidity of the surface.<sup>8</sup> Rustad et al. gave details about the pathways and explained why the exchange rates are so sensitive to single-atom substitutions.<sup>9</sup> Hunter and Ross found that  $\varepsilon\text{-K-Al}_{13}$  is more toxic than the monomer in forested spodosol soils.<sup>10</sup> Studies on the formation and evolution process of aqueous aluminum species are significant for a deep understanding of the action mechanism of polyaluminum flocculants on the surfaces of colloidal particles or for an objective selection of highly efficient and low toxicity flocculants in the water treatment field.<sup>4,11</sup>

For the study of aluminum species, many research methods are appropriate such as aluminum-ferrous complexation-timed spectrophotometry,<sup>12</sup>  $^{27}\text{Al}$  NMR spectrometry<sup>13</sup> and mass spectrometry.<sup>14</sup> However, a superior approach is to synthesize additional pure polyaluminum compounds, solve their crystal structures, characterize their properties, and relate them to each other.<sup>15</sup> Although polyaluminum species have been studied for about a century only eight species have been identified by crystal structure analysis.<sup>15–23</sup> A polyhedral representation (Supporting Information, Figure S1) and a classification of these structures

are given in the Supporting Information. To explain and predict the formation and transformation of various aqueous aluminum species two well-known but controversial polymerization models, the “core-links” model (also known as the “hexameric ring” model)<sup>24</sup> and the “cage-like”  $\text{K-Al}_{13}$  aggregation model,<sup>16</sup> have coexisted for 50 years. To unify the two models a “continuous” model has been proposed.<sup>2</sup> However, since the hydrolysis reaction process is complicated and only a few structures of hydrolyzates are known, a consensus has still not been reached and the hydrolytic chemistry of  $\text{Al}^{\text{III}}$  remains poorly understood.<sup>3,4</sup>

Our group has prepared more than 20 kinds of polyaluminum compounds<sup>25–34</sup> from hydrolyzed aluminum solutions, and their X-ray diffraction (XRD) patterns (Supporting Information, Figures S2–S3) are provided in the Supporting Information. Eight of these have been verified as new species while six of them were characterized by X-ray single crystal structure analysis.<sup>15,20</sup> In a previous paper, we divided all the structurally known polyaluminum species into “plank-suspending” (some  $\text{AlO}_6$  octahedra are connected to each other in a vertex- and edge-sharing manner to form a “plank” with some additional  $\text{AlO}_6$  octahedral monomers “suspended” on the periphery by vertex-sharing) and “core-shell” structures. We reported the structures of  $\text{S-K-Al}_{13}$  and  $\text{S-Al}_{32}$ , which are coordinated by sulfate ions in addition to  $\text{O}^{2-}$ ,  $\text{OH}^-$ , and  $\text{OH}_2$  ligands, and proposed an evolution mechanism from  $\varepsilon\text{-K-Al}_{13}$  to  $\text{S-K-Al}_{13}$  and  $\text{S-Al}_{32}$ .<sup>15</sup> In this paper, we report the structure of a new polyaluminum compound  $[\text{Al}_4(\text{OH})_6(\text{H}_2\text{O})_{12}][\text{Al}(\text{H}_2\text{O})_6]_2\text{Br}_{12}$ .

Received: February 9, 2011

Published: September 09, 2011

Table 1. Crystallographic Data and Structure Refinement Parameters

item	data	item	parameter
empirical formula	Al <sub>12</sub> Br <sub>24</sub> H <sub>108</sub> O <sub>60</sub>	limiting indices	−28 ≤ <i>h</i> ≤ +19
fw	3310.46		−28 ≤ <i>k</i> ≤ +27
temp (K)	100(2)		−27 ≤ <i>l</i> ≤ +28
cryst syst	cubic	θ range (deg)	1.68–28.32
space group	<i>Fd</i> $\bar{3}m$ (No. 227)	all/unique reflns/ <i>R</i> <sub>int</sub>	16411/600/0.0447
<i>a</i> (Å)	21.015(2)	completeness (%)	99.8
volume (Å <sup>3</sup> )	9281(3)	data/restraints/param	600/0/48
<i>Z</i>	4	obsd reflns [ <i>I</i> > 2σ( <i>I</i> )]	576
<i>D</i> <sub>c</sub> (g/cm <sup>3</sup> )	2.369	GOF on <i>F</i> <sup>2</sup> [ <i>I</i> > 2σ( <i>I</i> )]	1.074
<i>F</i> (000)	6336	GOF on <i>F</i> <sup>2</sup> (all data)	1.074
crystal size (mm <sup>3</sup> )	0.20 × 0.20 × 0.10	<i>R</i> indices [ <i>I</i> > 2σ( <i>I</i> )]	<i>R</i> <sub>1</sub> = 0.0328, <i>wR</i> <sub>2</sub> = 0.0878
abs coeff (mm <sup>−1</sup> )	10.549	<i>R</i> indices (all data)	<i>R</i> <sub>1</sub> = 0.0342, <i>wR</i> <sub>2</sub> = 0.0885
color	colorless	largest difference peak/hole (e/Å <sup>3</sup> )	0.938/−1.669
λ (Mo <i>K</i> <sub>α</sub> ) (Å)	0.71073	residual electron density (e/Å <sup>3</sup> )	0.121

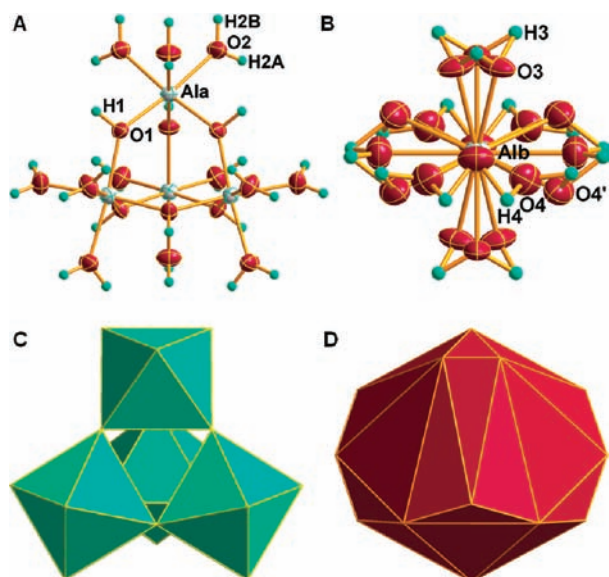


**Figure 1.** Ionic structures of  $[\text{Al}_4(\text{OH})_6(\text{H}_2\text{O})_{12}]^{6+}$  ( $\text{Al}_4$ ) and  $[\text{Al}(\text{H}_2\text{O})_6]^{3+}$  ( $\text{Al}_1$ ): (A and B) ellipsoid-stick representations with a probability of 80%, (C and D) polyhedral representations.

## EXPERIMENTAL DETAILS

**Synthesis.** A 41.25 g portion of  $\text{AlBr}_3 \cdot 6\text{H}_2\text{O}$  (A.R.) was dissolved in 58.0 mL of deionized water while stirring, and the solution was heated to 75 °C. A 0.72 g portion of Al powder (99.9%) was then added under fast stirring conditions. After complete dissolution the solution became clear and stirring was stopped. The temperature was maintained for 24 h. The solution obtained at a *B* of 0.585 ( $B = [\text{OH}]/[\text{Al}]$ ) was cooled to 50 °C, and the solvent water was allowed to slowly evaporate. After 21 d, colorless octahedral single crystals were obtained. This new polyaluminum bromide was also obtained by diluting 63.5 g of hydrobromic acid (40% HBr, A.R.) with 32.3 mL of deionized water and then adding 4.24 g of Al powder using the same procedure mentioned above. When most of the solvent water was evaporated from the solution obtained with a *B* of 1.00 the target compound was found to be of high purity and was isolated. The yield was as much as 83.0%. The synthesis experiment was repeated several times using different methods with a *B* range of 0.58–1.27. An almost pure product was obtained in each case.

**X-ray Crystal Structure Analysis.** Diffraction intensities were recorded on a Bruker SMART APEX-II X-ray diffractometer (graphite monochromator, CCD area detector). Multi-Scan absorption corrections were applied using the SADABS software program,<sup>35</sup> and diffraction data were reduced using the Bruker SAINT software program.<sup>36</sup> The initial structure was solved by “direct methods” using the SHELXS-97 software program,<sup>36</sup> and the coordinates of other non-hydrogen atoms were obtained from difference Fourier maps. All the coordinates and the anisotropic thermal parameters of the non-hydrogen atoms were refined by full-matrix least-squares techniques based on *F*<sup>2</sup> using the SHELXL-97 software program.<sup>36</sup> All the H atom or fragment coordinates were also obtained from difference Fourier maps and were refined without any restraint except for their isotropic thermal parameters. A thermogravimetric (TG) analysis of the compound (Supporting Information, Figure S5) was considered when assigning 1/3 to the occupancies of the disordered O and 2/3 to the corresponding H fragments. The crystallographic data and structure refinement parameters are listed in Table 1. The ionic structures of  $\text{Al}_4$  and  $\text{Al}_1$  are shown in Figure 1 and the crystal structure of  $[\text{Al}_4(\text{OH})_6(\text{H}_2\text{O})_{12}][\text{Al}(\text{H}_2\text{O})_6]_2\text{Br}_{12}$  is shown in Figure 2. The H bond system is shown in Supporting Information, Figure S4.

## RESULTS AND DISCUSSION

Two aluminum species, the tetramer  $[\text{Al}_4(\text{OH})_6(\text{H}_2\text{O})_{12}]^{6+}$  ( $\text{Al}_4$ ) and the monomer  $[\text{Al}(\text{H}_2\text{O})_6]^{3+}$  ( $\text{Al}_1$ ), are present in the structure of the compound, as shown in Figure 1. The tetramer comprises four identical distorted  $\text{AlO}_6$  octahedra that connect with each other by sharing three vertexes of each forming a large regular tetrahedron with ideal *T<sub>d</sub>* symmetry. The monomer is composed of a central  $\text{Al}^{3+}$  ion and 6 coordinated  $\text{OH}_2$  molecules in which the 6 O atoms are disordered into 18 O fragments with an identical occupancy of 1/3 and the 12 H atoms are disordered into 18 H fragments with an identical occupancy of 2/3. Twelve of the 18 O fragments form a waveform ring that surrounds the “equator” of which 6 O4 fragments are retained on a plane with an identical  $\text{Alb}-\text{O4}$  bond length of 1.873 Å and the 6 O4' fragments on the periphery of the plane at the upper and lower positions alternate with  $\text{Alb}-\text{O4}'$  bond lengths of 1.864 Å (see Figure 1B). The other 6 O3 fragments constitute two triangles that cover the two “poles” in a crosswise manner with an identical  $\text{Alb}-\text{O3}$  bond length of 1.859 Å. Each of the 18 H fragments is shared by two adjacent O fragments. Therefore, the original

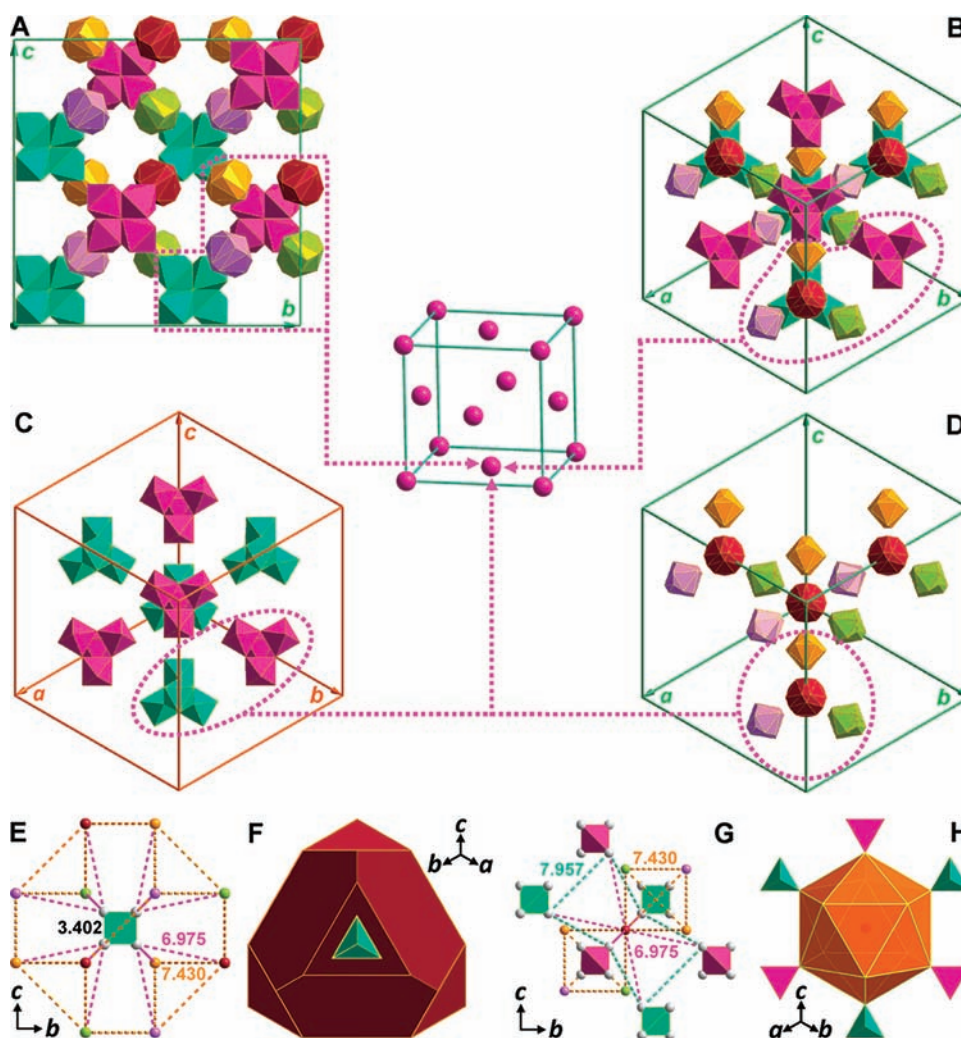


**Figure 2.** Crystal structure of  $[\text{Al}_4(\text{OH})_6(\text{H}_2\text{O})_{12}][\text{Al}(\text{H}_2\text{O})_6]_2\text{Br}_{12}$ : (A and B) Overall distribution of the 8  $\text{Al}_4$  and 16  $\text{Al}_1$  species in a unit cell viewed along the  $\{100\}$  (A) and  $\{111\}$  (B) direction; (C and D) Separate distribution of the 8  $\text{Al}_4$  (C) and 16  $\text{Al}_1$  (D) species in the same unit cell viewed along the  $\{111\}$  direction in which only 3 of the 12  $\text{Al}_1$  located at the edge-centered positions and 6 of the 12  $\text{Al}_1$  located on the six faces of the unit cell are drawn for clarity while the species with the same orientation have the same color (color code: cyan and magenta,  $\text{Al}_4$ ; amaranthine, light orange, lime, and lavender,  $\text{Al}_1$ ). The middle inset shows the face-centered lattice of the crystal and each lattice point represents 2  $\text{Al}_4$  species (in different orientations), 4  $\text{Al}_1$  species (in different orientations too) and 24  $\text{Br}^-$  anions (which are omitted for clarity) as outlined by the pink dashed lines in A or B, or C plus D. (E and G) are the shortest intra- and intermolecular  $\text{Al}\cdots\text{Al}$  distances around each  $\text{Al}_4$  (E) and  $\text{Al}_1$  (G) in which all the O and H atoms or fragments are omitted for clarity. Equal  $\text{Al}\cdots\text{Al}$  distances are marked with the same color dashed lines while the four gray balls on the vertexes of the regular tetrahedron represent the four  $\text{Al}^{3+}$  members of  $\text{Al}_4$ . Each of the colored balls represents the central  $\text{Al}^{3+}$  of an  $\text{Al}_1$  species and its color corresponds with that of its coordinated polyhedron in A, B, and D. (F and H) are the polyhedral distributions of the nearest 12  $\text{Al}_1$  species around each  $\text{Al}_4$  (F) species and the nearest 6  $\text{Al}_4$  species in addition to the slightly longer 6  $\text{Al}_1$  species around each  $\text{Al}_1$  (H) species.

regular octahedral  $\text{Al}(\text{H}_2\text{O})_6^{3+}$  monomer with ideal  $O_h$  symmetry is disordered into a core–shell structure with ideal  $D_{3d}$  symmetry for this polyaluminum bromide.

From Figure 2A–D it is clear that two kinds of aluminum species ( $\text{Al}_4$  and  $\text{Al}_1$ ) coexist in a ratio of 1:2 in each unit cell. In total there are 8  $\text{Al}_4$ , 16  $\text{Al}_1$  species, and 96  $\text{Br}^-$  anions in a unit cell. The 8  $\text{Al}_4$  tetramers fall into two groups with opposite orientation (4 cyan and 4 magenta) and the distribution of their barycenters is similar to that of the 8 C atoms in diamond (see Figure 2C). The 16  $\text{Al}_1$  monomers fall into four groups with different orientations: The 4 amaranthine monomers are respectively located at the body-centered ( $1/2, 1/2, 1/2$ ) and the edge-centered positions ( $1/2, 1, 1$ ;  $1, 1/2, 1$ ;  $1, 1, 1/2$ ); the 4 light orange monomers are respectively located at the diagonals (which do

not cross the  $c$  axis) of the (001) faces ( $3/4, 1/4, 1$ ;  $1/4, 3/4, 1$ ) and the diagonals (which cross the  $c$  axis) of the (002) planes ( $1/4, 1/4, 1/2$ ;  $3/4, 3/4, 1/2$ ); similarly, the 4 lime monomers are at the diagonals of the (010) faces ( $3/4, 1, 1/4$ ;  $1/4, 1, 3/4$ ) and the (020) planes ( $1/4, 1/2, 1/4$ ;  $3/4, 1/2, 3/4$ ) while the 4 lavender monomers are at the diagonals of the (100) faces ( $1, 3/4, 1/4$ ;  $1, 1/4, 3/4$ ) and the (200) planes ( $1/2, 1/4, 1/4$ ;  $1/2, 3/4, 3/4$ ) (see Figure 2D). The 96  $\text{Br}^-$  anions fall into four groups [16  $\text{Br}_1$ , 32  $\text{Br}_2$ , 48  $\text{Br}_3$  (occupancy 1/2) and 96  $\text{Br}_3'$  (occupancy 1/4)], and they are interspersed among the interstices between the  $\text{Al}_4$  and  $\text{Al}_1$  species that have fixed positions after the formation of strong hydrogen bonds with  $\text{OH}\cdots\text{Br}$  bond lengths ranging from 2.32 to 2.57 Å, as shown in Supporting Information, Figure S4.



From the middle inset it is obvious that 2  $\text{Al}_4$  species, 4  $\text{Al}_1$  species and 24  $\text{Br}^-$  anions constitute a structural motif (a lattice point) as outlined by the pink dashed lines in Figure 2A, Figure 2B, Figure 2C and Figure 2D. That is, a lattice point represents 2  $[\text{Al}_4(\text{OH})_6(\text{H}_2\text{O})_{12}][\text{Al}(\text{OH}_2)_6]_2\text{Br}_{12}$  molecules with different orientations. Thus, the 8  $[\text{Al}_4(\text{OH})_6(\text{H}_2\text{O})_{12}][\text{Al}(\text{OH}_2)_6]_2\text{Br}_{12}$  molecules in each unit cell form a face-centered cubic lattice ( $Z = 4$ ).

The intermolecular contacts around each  $\text{Al}_4$  and  $\text{Al}_1$  species are shown in Figure 2E–H. It is clear that each  $\text{Al}_4$  (intramolecular  $\text{Ala}\cdots\text{Ala}$  distances are 3.402 Å) tetrahedron is surrounded by 12 of the nearest disordered  $\text{Al}(\text{OH}_2)_6^{3+}$  monomers ( $\text{Al}_1$ ) with equivalent intermolecular  $\text{Ala}\cdots\text{Alb}$  distances of 6.975 Å (see Figure 2E). They form a core–shell structure (see Figure 2F), and it is similar to the well-known structure of Keggin- $\text{Al}_{13}$  (see also Supporting Information, Figure S1). Each  $\text{Al}_1$  is surrounded by 6 of the nearest  $\text{Al}_4$  species with equivalent intermolecular  $\text{Alb}\cdots\text{Ala}$  distances of 6.975 Å and 6 of slightly longer  $\text{Al}_1$  species with equivalent intermolecular  $\text{Alb}\cdots\text{Alb}$  distances of 7.430 Å (see Figure 2G, the shortest intermolecular  $\text{Ala}\cdots\text{Ala}$  distances are 7.957 Å). A distorted icosahedron is formed in which 2 of the 20 triangles are equilateral (see Figure 2H). No direct contact is evident between the  $\text{Al}_4$  and  $\text{Al}_1$  species, and all the intermolecular contacts mentioned above are via  $\text{Br}^-$  anions that are located between them and they form a complicated H bond system (see also Supporting Information, Figure S4).

Because of the appearance of tetrahedral  $[\text{Al}_4(\text{OH})_6(\text{H}_2\text{O})_{12}]^{6+}$  and disordered  $[\text{Al}(\text{OH}_2)_6]^{3+}$  that coexist in a 1:2 ratio in each unit cell we obtained new information.

First, the presence of the tetrahedral  $\text{Al}_4$  species was completely unexpected in terms of current polymerization models such as the “hexameric ring” model, the “cage-like”  $\text{K}-\text{Al}_{13}$  aggregation model, and the “continuous” model. The “hexameric ring” model describes the whole hydrolysis-polymerization process from the monomer to the polymer in addition to  $\text{Al}(\text{OH})_3$  precipitation, which maintains the sheet structure of gibbsite or bayerite, and this develops continuously from the basic hexameric ring unit.<sup>24</sup> However, the  $\text{Al}_4$  species has a stereoscopic tetrahedral configuration. In the “cage-like”  $\text{K}-\text{Al}_{13}$  aggregation model several dominant species transform each other directly in the hydrolyzed aluminum solution in addition to the monomer and the dimer. Only  $\text{K}-\text{Al}_{13}$  and its aggregates can exist, and they are characterized by a “core-shell” structure.<sup>16</sup> However, no  $\text{AlO}_4$  core in the  $\text{Al}_4$  species is predicted. The “continuous” model<sup>2</sup> is a unification of the two above-mentioned models, and it still describes an evolution process from a small polymer (linear shape) to a middle-sized polymer (plane shape) and a large polymer (stereoscopic conformation), as suggested by the “hexameric ring” model, but it cannot explain why the small  $\text{Al}_4$  species has a stereoscopic structure. This implies that a new evolution model and theory is required, and this will be reported later.

Second, the four  $\text{AlO}_6$  octahedra that connect with each other by vertex-sharing giving a large regular tetrahedron with the highest  $T_d$  symmetry has not been reported to date for any polyaluminum species or for any aluminiferous minerals found in the earth's crust. One slightly similar example may be found in work done on antimonite acid in which four  $\text{SbO}_6$  octahedra were found to be connected to each other by vertex-sharing resulting in the formation of a large distorted tetrahedral  $\text{Sb}_4\text{O}_2(\text{OH})_{16}$

unit, and it further connects to others by vertex-sharing resulting in a pyrochlorite structure.<sup>5</sup>

Third, solvent molecules or counterions are often disordered especially when they are placed near or on a symmetry element; however, a regular octahedral  $\text{Al}(\text{H}_2\text{O})_6^{3+}$  monomer with  $O_h$  symmetry has never been observed as a disordered core–shell structure with  $D_{3d}$  symmetry (see Figure 1B). This indicates that strong interactions exist among the  $\text{Al}_4$  species,  $\text{Al}_1$  species and the  $\text{Br}^-$  anions (see also Supporting Information, Figure S4).

Finally, two or more different simple metal cations often occupy respective positions in a crystal lattice such as perovskite-type  $\text{CaTiO}_3$ ,  $\text{Ba}(\text{Fe}_{0.5}\text{Ta}_{0.5})\text{O}_3$ , and superconducting  $\text{La}_2\text{CuO}_4$ ,  $\text{YBa}_2\text{Cu}_3\text{O}_6$ , and  $\text{YBa}_2\text{Cu}_3\text{O}_7$ .<sup>37</sup> However, the coexistence of two different aluminum species in a polyaluminum compound has never been observed. The coexistence of  $\text{Al}_4$  and  $\text{Al}_1$  in a lattice structure reflects the ubiquity of aluminum monomers in solution indicating that aluminum monomers may always be present in a hydrolyzed aluminum solution because it is still a required participator in the formation processes of  $\text{Al}_{30}$  and  $\text{S}-\text{Al}_{32}$ , even under a higher degree of medium basification (such as  $B = 2.5$ ).<sup>38,15</sup>

## CONCLUSION

A vertex-shared tetrahedral aluminum tetramer  $[\text{Al}_4(\text{OH})_6(\text{H}_2\text{O})_{12}]^{6+}$  ( $\text{Al}_4$ ) and a disordered core–shell aluminum monomer  $[\text{Al}(\text{OH}_2)_6]^{3+}$  ( $\text{Al}_1$ ) were found in a new polyaluminum bromide  $[\text{Al}_4(\text{OH})_6(\text{H}_2\text{O})_{12}][\text{Al}(\text{H}_2\text{O})_6]_2\text{Br}_{12}$  that was crystallized from a spontaneously hydrolyzed solution of  $\text{AlBr}_3$ . They coexist in the crystal lattice of the cubic system with a  $Fd\bar{3}m$  space group and a 1:2 molar ratio. The former is the smallest known stereoscopic aluminum species. Their ionic and crystal structures are described, and their structural features are discussed. We believe that the discovery of the vertex-shared tetrahedral aluminum tetramer is very important for a deeper understanding of the formation and evolution process of aluminum species and for improving the current polymerization models in hydrolyzed aluminum solutions. These findings greatly impact many natural science related fields where the hydrolysis chemistry of  $\text{Al}^{\text{III}}$  is of interest such as geochemistry, environmental science, biochemistry, medicine, and water treatment.

## ASSOCIATED CONTENT

**S Supporting Information.** Crystallographic data in CIF format for  $\text{Al}_6(\text{OH})_6(\text{H}_2\text{O})_{24}\text{Br}_{12}$ , the structurally known polyaluminum species (Figure S1) and their classification, the XRD patterns of the polyaluminum compounds prepared by our group (Figures S2–S3), the H bond system around each  $\text{Br}^-$  anion (Figure S4), and the characterization results from other methods (TA, Figure S5; XRD, Figure S6; and FT-IR, Figure S7).<sup>39–41</sup> This material is available free of charge via the Internet at <http://pubs.acs.org>. The CIF may also be obtained from Fachinformationszentrum Karlsruhe, 76344 Eggenstein-Leopoldshafen, Germany [fax (+49)7247–808–666; e-mail [crysdata@fiz-karlsruhe.de](mailto:crysdata@fiz-karlsruhe.de); Web site [http://www.fiz-karlsruhe.de/request\\_for\\_deposited\\_data.html](http://www.fiz-karlsruhe.de/request_for_deposited_data.html)] upon quoting the depository number CSD 380483.

## AUTHOR INFORMATION

### Corresponding Author

\*E-mail: [cesz2008@126.com](mailto:cesz2008@126.com). Fax: +86 471 4992981.

## ACKNOWLEDGMENT

We are thankful for support from the National Natural Science Foundation Committee of China [NNSFC Grants 20563002 (to Z.S.) and 20967005 (to H.W.)].

## REFERENCES

- (1) Casey, W. H. *Chem. Rev.* **2006**, *106*, 1–16.
- (2) Bi, S. P.; Wang, C. Y.; Cao, Q.; Zhang, C. H. *Coord. Chem. Rev.* **2004**, *248*, 441–455.
- (3) Swaddle, T. W.; Rosenqvist, J.; Yu, P.; Bylaska, E.; Phillips, B. L.; Casey, W. H. *Science* **2005**, *308*, 1450–1453.
- (4) Tang, H. X. *Inorganic Polymer Flocculation Theory and Flocculants*; China Architecture & Building Press: Beijing, China, 2006.
- (5) Jolivet, J. P.; Henry, M.; Livage, J. *Metal Oxide Chemistry and Synthesis: From Solution to Solid State*; John Wiley & Sons: Chichester, U.K., 2000.
- (6) Bertsch, P. M.; Parker, D. R. *Aqueous Polynuclear Aluminum Species: The Environmental Chemistry of Aluminum*, 2nd ed.; CRC Press: Boca Raton, FL, 1996.
- (7) Furrer, G.; Phillips, B. L.; Ulrich, K. -U.; Pöthig, R.; Casey, W. H. *Science* **2002**, *297*, 2245–2247.
- (8) Phillips, B. L.; Casey, W. H.; Karlsson, M. *Nature* **2000**, *404*, 379–382.
- (9) Rustad, J. R.; Loring, J. S.; Casey, W. H. *Geochim. Cosmochim. Acta* **2004**, *68*, 3011–3017.
- (10) Hunter, D.; Ross, D. S. *Science* **1991**, *251*, 1056–1058.
- (11) Stewart, T. A.; Trudell, D. E.; Alam, T. M.; Ohlin, C. A.; Lawler, C.; Casey, W. H.; Jett, S.; Nyman, M. *Environ. Sci. Technol.* **2009**, *43*, 5416–5422.
- (12) Smith, R. W. *Adv. Chem. Ser.* **1971**, *106*, 250–256.
- (13) Allouche, L.; Huguenard, C.; Taulelle, F. *J. Phys. Chem. Solids* **2001**, *62*, 1525–1531.
- (14) Lin, Y. -F.; Lee, D. -J. *J. Phys. Chem. A* **2010**, *114*, 3503–3509.
- (15) Sun, Z.; Wang, H.; Tong, H. G. E.; Sun, S. F. *Inorg. Chem.* **2011**, *50*, 559–564.
- (16) (a) Johansson, G. *Acta Chem. Scand.* **1960**, *14*, 771–773. (b) Johansson, G.; Lundgren, G.; Sillén, L. G.; Söderquist, R. *Acta Chem. Scand.* **1960**, *14*, 769–771. (c) Johansson, G. *Ark. Kemi* **1963**, *20*, 305–319, 321–342.
- (17) Rowsell, J.; Nazar, L. F. *J. Am. Chem. Soc.* **2000**, *122*, 3777–3778.
- (18) Allouche, L.; Gérardin, C.; Loiseau, T.; Férey, G.; Taulelle, F. *Angew. Chem., Int. Ed.* **2000**, *39*, 511–514.
- (19) Seichter, W.; Mögel, H. J.; Brand, P.; Salah, D. *Eur. J. Inorg. Chem.* **1998**, 795–797.
- (20) Sun, Z.; Zhao, H. D.; Tong, H. G. E.; Wang, R. F.; Zhu, F. Z. *Chin. J. Struct. Chem.* **2006**, *25*, 1217–1227.
- (21) Gatlin, J. T.; Mensinger, Z. L.; Zakharov, L. N.; MacInnes, D.; Johnson, D. W. *Inorg. Chem.* **2008**, *47*, 1267–1269.
- (22) Casey, W. H.; Olmstead, M. M.; Phillips, B. L. *Inorg. Chem.* **2005**, *44*, 4888–4890.
- (23) Johansson, G. *Acta Chem. Scand.* **1962**, *16*, 403–420.
- (24) (a) Brosset, C. *Acta Chem. Scand.* **1952**, *6*, 910–940. (b) Brosset, C.; Biedermann, G.; Sillén, L. G. *Acta Chem. Scand.* **1954**, *8*, 1917–1926. (c) Sillén, L. G. *Acta Chem. Scand.* **1954**, *8*, 299–317. (d) Hsu, P. H.; Rich, C. I. *Soil Sci. Soc. Am. Proc.* **1960**, *24*, 21–25. (e) Hsu, P. H.; Bates, T. F. *Mineral. Mag.* **1964**, *33*, 749–768. (f) Stol, R. J.; Van Helden, A. K.; De Bruyn, P. L. *J. Colloid Interface Sci.* **1976**, *57*, 115–131.
- (25) Du, S. Y.; Wang, H.; Sun, Z. *J. Environ. Sci. Eng.* **2009**, *3*, 47–52.
- (26) Du, S. Y.; Sun, Z.; Wang, H. *J. Chem. Chem. Eng.* **2008**, *2*, 16–19.
- (27) Wang, R. F.; Sun, Z.; Zhang, Y. *Chin. J. Appl. Chem.* **2009**, *26*, 878–880.
- (28) Sun, Z. Chinese Invention Patent ZL200510064782.6, 2007.
- (29) Sun, Z.; Zhao, H. D.; Yang, X. S.; Zhu, F. Z. *Chin. J. Environ. Chem.* **2007**, *26*, 31–34.
- (30) Fei, Y. L.; Sun, Z.; Wang, R. F.; Tong, H. G. E.; Zhang, B. L. C. *Nat. Sci. Res.* **2007**, *10*, 65–67.
- (31) Du, S. Y.; Sun, Z.; Wang, H. *J. Environ. Sci. Eng.* **2008**, *2*, 30–32.
- (32) Meng, Y. F.; Sun, Z.; Wang, H.; Yu, N. N. *J. Environ. Sci. Eng.* **2008**, *2*, 15–17.
- (33) Du, S. Y.; Sun, Z.; Wang, H. *J. Environ. Sci. Eng.* **2009**, *3*, 40–42, 52.
- (34) Meng, Y. F.; Sun, Z.; Wang, H.; Feng, H. J. *J. Chem. Chem. Eng.* **2008**, *2*, 25–28.
- (35) Sheldrick, G. M. *SADABS: Siemens Area Detector Absorption Correction*; University of Göttingen: Göttingen, Germany, 2008.
- (36) Sheldrick, G. M. *SHELXTL*; Bruker Analytical X-ray Systems: Madison, WI, 2008.
- (37) Zhou, G. D.; Duan, L. Y. *Foundation of Structural Chemistry*, 4th ed.; Peking University Press: Beijing, China, 2008.
- (38) Allouche, L.; Taulelle, F. *Inorg. Chem. Commun.* **2003**, *6*, 1167–1170.
- (39) Ning, X. A.; Li, K.; Li, R. S.; Wen, Y. M. *Chin. J. Environ. Chem.* **2008**, *27*, 263–264.
- (40) Chen, W. N.; Zhong, H. P.; Yang, J.; Chen, Y. J.; Li, L. *Chin. J. Chem. Res. Appl.* **2002**, *14*, 73–75.
- (41) Zhao, H. Z.; Peng, J. X.; Lin, S. S.; Zhang, Y. *Environ. Sci. Technol.* **2009**, *43*, 2041–2046.